Structural Engineering and Mechanics, *Vol. 54, No. 4 (2015) 649-664*
DOI: http://dx.doi.org/10.12989/sem.2015.54.4.649

Analytical solution for axisymmetric buckling of joined conical shells under axial compression

M.A. Kouchakzadeh[*1] and M. Shakouri[2a]

[1]*Department of Aerospace Engineering and Center of Excellence in Aerospace Systems, Sharif University of Technology, P.O. Box 11155-8639, Tehran, Iran*
[2]*Department of Aerospace Engineering, Sharif University of Technology, P.O. Box 11155-8639, Tehran, Iran*

(Received April 3, 2014, Revised october 12, 2014, Accepted November 22, 2014)

Abstract. In this study, the authors present an analytical approach to find the axisymmetric buckling load of two joined isotropic conical shells under axial compression. The problem of two joined conical shells may be considered as the generalized form of joined cylindrical and conical shells with constant or stepped thicknesses. Thickness of each cone is constant; however it may be different from the thickness of the other cone. The boundary conditions are assumed to be simply supported with rigid rings. The governing equations for the conical shells are obtained and solved with an analytical approach. A simple closed-form expression is obtained for the buckling load of two joined truncated conical shells. Results are compared and validated with the numerical results of finite element method. The variation of buckling load with changes in the thickness and semi-vertex angles of the two cones is studied. Finally, application of the results in practical design and range of engineering validity are investigated.

Keywords: joined conical shells; buckling; analytical solution; design application

1. Introduction

The joined shells of revolution (such as cone-cone, cone-cylinder, sphere-cylinder, …) have many applications in tanks and pressure vessels, jet nozzles and many other cases in civil, mechanical, aeronautical, marine and power engineering. They may consist of thin-walled structures composed of two or more simple components having one axis of revolution and slope discontinuity in the shell meridian.

Buckling and instability of conical shells –as an important failure mode- has attracted the attention of many investigators. One of the earliest works on buckling of conical shells was published by Seide (1956). He developed a simple closed form solution for axisymmetric buckling of conical shells under axial compression. This expression is used as the classical buckling load for axially compressed conical shells till now. The applicability of Seide's formula was verified with the experiments performed by Lackman and Penzien (1960). The elastic stability of truncated conical shells under axial compression for simply-supported and clamped boundary conditions is

∗Corresponding author, Ph.D., E-mail: mak@sharif.edu
[a]Ph.D. Student, E-mail: shakouri@ae.sharif.edu

http://www.techno-press.org/?journal=sem&subpage=8 ISSN: 1225-4568 (Print), 1598-6217 (Online)

investigated by (Tani and Yamaki 1970). In recent years, there are many investigations on the buckling of truncated conical shells made up of composites (Sofiyev 2003, Shadmehri *et al*. 2012) and Functionally Graded Materials (FGMs) (Sofiyev 2011) and a wide range of loading types such as axial load (Gupta *et al*. 2006, Sofiyev 2007, Sofiyev 2011), hydrostatic pressure (Ross *et al*. 1999, Ross *et al*. 2005, Hafeez *et al*. 2010) and combined loads (Sofiyev 2010). A comprehensive review on the problem of buckling of moderately thick, laminated, composite shells subjected to uniform axial compression, uniform lateral pressure and torsion applied individually or in combination was done by (Simitses 1996). Effects of shear loads on vibration and buckling of anti-symmetric cross-ply cylindrical panels was studied by (Hui 1988) and the discrete singular Convolution (DSC) technique was employed to study the buckling and vibration behavior of cylindrical and conical shells (Civalek and Gürses 2009, Civalek 2013).

The buckling of joined shells has been studied by many researchers. Teng and his colleagues (Teng 1996, Teng and Barbagallo 1997, Teng and Ma 1999, Zhao and Teng 2003) studied the elastic buckling and post-buckling of joined conical-cylindrical shells subjected to internal pressure. Flores and Godoy (1991) used finite element method to study the elastic buckling and post-buckling of cone-cylinder and sphere-cylinder joined shells subjected to external pressure. The results show that the bifurcation loads of the complex shells are lower than those of the individual components. The plastic buckling analysis of thick isotropic cone-cylinder and spherical cap-cylinder shells is studied by (Bushnell and Galletly 1974). Kamat *et al*. (2001) used finite element method and first ordered shear deformation theory to analyze the dynamic instability of a joined conical-cylindrical shell subjected to periodic in-plane load.

Patel and his colleagues (Patel *et al*. 2005; Patel *et al*. 2006; Patel *et al*. 2008) studied the nonlinear thermo-elastic buckling and post-buckling characteristics of laminated conical-cylindrical and conical-cylindrical-conical joined shells subjected to uniform temperature rise. The problem of liquid filled joined conical shells is studied by Zingoni (2002, 2004) and discontinuity of stresses in shell intersection is investigated. Also, Anwen (1998) showed that the insertion of a toroidal segment in joint area of the cone and cylinder results in slightly higher external buckling pressures than that of cone–cylinder shell without transition. The buckling of joined shells with different geometries are investigated by many researchers as mentioned above, however, there are just a few studies available on the characteristics of two joined conical shells.

The problem of two joined conical shells may be considered as the generalized form for the problem of one conical shell with stepped thickness, joined conical-cylindrical shells and joined cylindrical shells and flat end plates (Kouchakzadeh and Shakouri 2014). Therefore the buckling load of these special cases will be available as the result of this study.

In this study, the authors present an analytical approach to find the axisymmetric buckling load of two joined isotropic conical shells under axial compression. The governing equations for the conical shells are obtained and solved as described by Seide (1956). The boundary condition is assumed to be simply supported with rigid ring. A simple closed-form expression is obtained for the buckling load of two joined truncated cones with constant thicknesses and the results are compared and validated with the numerical results of finite element method. This expression is a good handy relation to be used in preliminary design procedure. For this application, the range of validity of this expression is obtained using finite element method.

As mentioned above, a closed form solution is obtained using analytical procedure. This analytical approach has the following advantages:

• The analytical methods generally enable us to have parametric studies more easily. Using these methods, effects of any parameter on the objective value (here the buckling load) may be

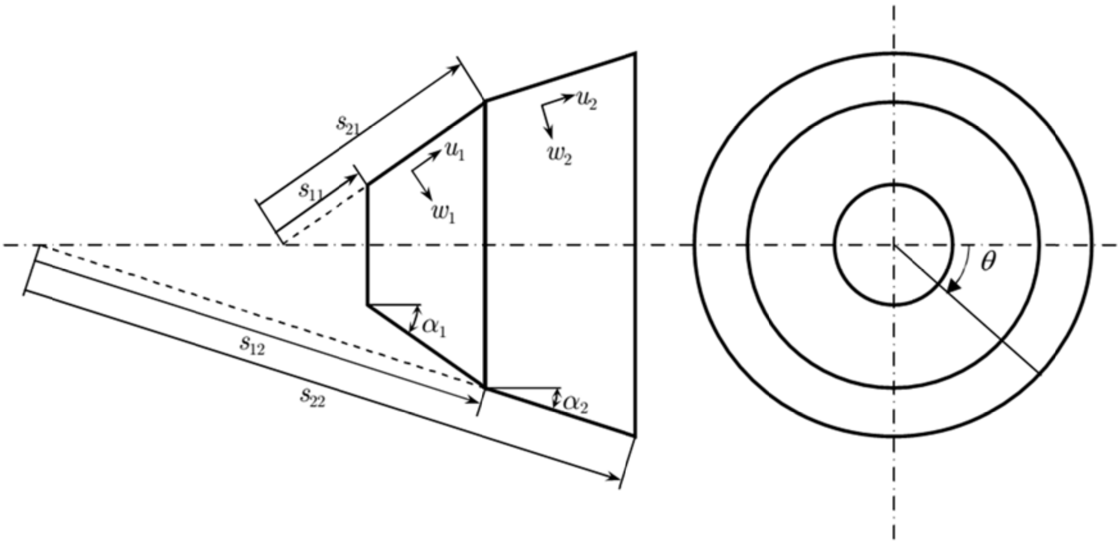

Fig. 1 Geometry of joined conical shells

obtained explicitly.

• Closed form results are very useful hand-calculating relations in preliminary design processes.

• Although the analytical formulas usually are obtained after some simplifying assumptions, the form of the relation between parameters can be employed to construct empirical, experimentally verified formulas with adding some constant values.

2. Governing equations for conical shells

For two joined conical shells, the coordinate system (s, θ) is defined in Fig. 1. The governing equations are given in terms of u and w that are the components of the displacement in the s and θ directions, respectively. α is the semi-vertex angle of the cone, L_1 and L_2 are the cone lengths, R is the radius at s_{11} and P is the axial load.

The governing equations can be derived according to the thin shell theory of Donnell type described by Seide (1956).

$$
\begin{aligned}
&(sN_s)_{,s} - N_\theta = 0 \\
&\frac{d}{ds}\left(\frac{-P}{\pi \sin 2\alpha}\frac{dw}{ds}\right) + N_\theta \cot\alpha + \frac{d}{ds}\left(sQ_s\right) = 0 \\
&\frac{d}{ds}\left(sM_s\right) - M_\theta - sQ_s = 0
\end{aligned}
\tag{1}
$$

Where N_s, M_s and Q_s are force, moment and shear stress resultants in s direction, respectively and N_θ, M_θ are force and moment resultants in θ direction, respectively. Here, only first-order terms have been included and the vertical component of the edge stress is assumed not to change after buckling. Stress-strain relations are given by

$$
\begin{aligned}
N_s &= C\left[\varepsilon_s + \nu\,\varepsilon_\theta\right] \\
N_\theta &= C\left[\varepsilon_\theta + \nu\,\varepsilon_s\right] \\
M_s &= D\left[\kappa_s + \nu\,\kappa_\theta\right] \\
M_\theta &= D\left[\kappa_\theta + \nu\,\kappa_s\right]
\end{aligned}
\tag{2}
$$

where ε and κ are the middle surface strain and the change in curvature due to buckling and given as

$$
\begin{aligned}
\varepsilon_s &= \frac{du}{ds} \\
\varepsilon_\theta &= \frac{u - w\cot\alpha}{s} \\
\kappa_s &= -\frac{d^2 w}{ds^2} \\
\kappa_\theta &= -\frac{1}{s}\frac{dw}{ds}
\end{aligned}
\tag{3}
$$

where u and w are middle surface displacements of cone in the direction and normal to cone generator due to buckling. Also, D and C are bending and extensional stiffness parameters and defined as

$$
\begin{aligned}
C &= \frac{E\,h}{1-\nu^2} \\
D &= \frac{E\,h^3}{12(1-\nu^2)}
\end{aligned}
\tag{4}
$$

where E is the elastic modulus, υ is Poisson's ratio and h is the shell thickness. Substitution of Eqs. (2) to (4) into Eq. (1) and some mathematical operations yields the closed-form equations for displacement u and w

$$
\begin{aligned}
u = 2\cot\alpha[C_1 &\left\{2\frac{J_1\left[2\sqrt{b_1 s}\right]}{2\sqrt{b_1 s}} + \nu J_2\left[2\sqrt{b_1 s}\right]\right\} + C_2\left\{2\frac{Y_1\left[2\sqrt{b_1 s}\right]}{2\sqrt{b_1 s}} + \nu Y_2\left[2\sqrt{b_1 s}\right]\right\} \\
&+ C_3\left\{2\frac{J_1\left[2\sqrt{b_2 s}\right]}{2\sqrt{b_2 s}} + \nu J_2\left[2\sqrt{b_2 s}\right]\right\} + C_4\left\{2\frac{Y_1\left[2\sqrt{b_2 s}\right]}{2\sqrt{b_2 s}} + \nu Y_2\left[2\sqrt{b_2 s}\right]\right\}]
\end{aligned}
\tag{5}
$$

$$
\begin{aligned}
w = C_1&\left\{2J_0\left[2\sqrt{b_1 s}\right] + \left[2\sqrt{b_1 s}\right]J_1\left[2\sqrt{b_1 s}\right]\right\} + C_2\left\{2Y_0\left[2\sqrt{b_1 s}\right] + \left[2\sqrt{b_1 s}\right]Y_1\left[2\sqrt{b_1 s}\right]\right\} \\
&+ C_3\left\{2J_0\left[2\sqrt{b_2 s}\right] + \left[2\sqrt{b_2 s}\right]J_1\left[2\sqrt{b_2 s}\right]\right\} + C_4\left\{2Y_0\left[2\sqrt{b_2 s}\right] + \left[2\sqrt{b_2 s}\right]Y_1\left[2\sqrt{b_1 s}\right]\right\}
\end{aligned}
\tag{6}
$$

where $J_n(x)$ and $Y_n(x)$ are Bessel functions of the first and second kinds, respectively and

$$
b_{1,2} = \frac{P}{2\pi D\sin 2\alpha}\left[1 \pm \sqrt{1 - \left(\frac{2Eh^2\pi}{P\sqrt{3(1-\nu^2)}}\cos^2\alpha\right)^2}\,\right]
\tag{7}
$$

2.1 Boundary and continuity conditions

Boundary conditions for the case of simply support and rigid rings at the edges are (Seide 1956)

$$\begin{cases} \dfrac{d^2 w}{ds^2} + \dfrac{\nu}{s}\dfrac{dw}{ds} = 0 \\ u \sin\alpha - w\cos\alpha = 0 \end{cases} \qquad \text{at} \quad s = s_{11}, s_{22} \tag{8}$$

To maintain the continuity at the junction of the two cones we have (Ventsel and Krauthammer 2001)

$$\begin{aligned} &\beta_{s1}(s_{12}) = \beta_{s2}(s_{21}) \\ &u_1(s_{12})\sin\alpha_1 - w_1(s_{12})\cos\alpha_1 = u_2(s_{21})\sin\alpha_2 - w_2(s_{21})\cos\alpha_2 \\ &M_{s1}(s_{12}) = M_{s2}(s_{21}) \\ &N_{\theta 1}(s_{12}) = N_{\theta 2}(s_{21}) \end{aligned} \tag{9}$$

Where β_s is the rotation of cone in s direction and described as

$$\beta_s(s) = -\frac{dw}{ds} \tag{10}$$

3. Solution

Substitution of Eqs. (5) and (6) into the boundary (8) and continuity (9) conditions, after some manipulation, yields the following criterion for instability of cones

$$\begin{vmatrix} [A]_{4\times4} & [B]_{4\times4} \\ [E]_{4\times4} & [F]_{4\times4} \end{vmatrix} = 0 \tag{11}$$

where

$$A = \left[\begin{matrix} (2\sqrt{b_{11}s_{11}})^3 J_2'(2\sqrt{b_{11}s_{11}}) + 2\nu(2\sqrt{b_{11}s_{11}})^2 J_2(2\sqrt{b_{11}s_{11}}) & (2\sqrt{b_{11}s_{11}})^3 Y_2'(2\sqrt{b_{11}s_{11}}) + 2\nu(2\sqrt{b_{11}s_{11}})^2 Y_2(2\sqrt{b_{11}s_{11}}) \\ 2\sqrt{b_{11}s_{11}} J_2'(2\sqrt{b_{11}s_{11}}) - 2\nu J_2(2\sqrt{b_{11}s_{11}}) & 2\sqrt{b_{11}s_{11}} Y_2'(2\sqrt{b_{11}s_{11}}) - 2\nu Y_2(2\sqrt{b_{11}s_{11}}) \\ \dfrac{b_{11}^2}{2\sqrt{b_{11}s_{21}}} J_2'(2\sqrt{b_{11}s_{21}}) & \dfrac{b_{11}^2}{2\sqrt{b_{11}s_{21}}} Y_2'(2\sqrt{b_{11}s_{21}}) \\ \left[2\sqrt{b_{11}s_{21}} J_2'(2\sqrt{b_{11}s_{21}}) - 2\nu J_2(2\sqrt{b_{11}s_{21}})\right]\cos\alpha_1 & \left[2\sqrt{b_{11}s_{21}} Y_2'(2\sqrt{b_{11}s_{21}}) - 2\nu Y_2(2\sqrt{b_{11}s_{21}})\right]\cos\alpha_1 \end{matrix}\right.$$

$$\left.\begin{matrix} (2\sqrt{b_{21}s_{11}})^3 J_2'(2\sqrt{b_{21}s_{11}}) + 2\nu x_{21}^{1\ 2} J_2(2\sqrt{b_{21}s_{11}}) & (2\sqrt{b_{21}s_{11}})^3 Y_2'(2\sqrt{b_{21}s_{11}}) + 2\nu(2\sqrt{b_{21}s_{11}})^2 Y_2(2\sqrt{b_{21}s_{11}}) \\ 2\sqrt{b_{21}s_{11}} J_2'(2\sqrt{b_{21}s_{11}}) - 2\nu J_2(2\sqrt{b_{21}s_{11}}) & 2\sqrt{b_{21}s_{11}} Y_2'(2\sqrt{b_{21}s_{11}}) - 2\nu Y_2(2\sqrt{b_{21}s_{11}}) \\ \dfrac{b_{21}^2}{2\sqrt{b_{21}s_{21}}} J_2'(2\sqrt{b_{21}s_{21}}) & \dfrac{b_{21}^2}{2\sqrt{b_{21}s_{21}}} Y_2'(2\sqrt{b_{21}s_{21}}) \\ \left[2\sqrt{b_{21}s_{21}} J_2'(2\sqrt{b_{21}s_{21}}) - 2\nu J_2(2\sqrt{b_{21}s_{21}})\right]\cos\alpha_1 & \left[2\sqrt{b_{21}s_{21}} Y_2'(2\sqrt{b_{21}s_{21}}) - 2\nu Y_2(2\sqrt{b_{21}s_{21}})\right]\cos\alpha_1 \end{matrix}\right] \tag{12}$$

$$B=\begin{bmatrix} 0 & 0 & 0 & 0 \\ 0 & 0 & 0 & 0 \\ -\frac{b_{12}^2}{2\sqrt{b_{12}s_{12}}}J_2'(2\sqrt{b_{12}s_{12}}) & -\frac{b_{12}^2}{2\sqrt{b_{12}s_{12}}}Y_2'(2\sqrt{b_{12}s_{12}}) & \frac{b_{22}^2}{2\sqrt{b_{22}s_{12}}}J_2'(2\sqrt{b_{22}s_{12}}) & \frac{b_{22}^2}{2\sqrt{b_{22}s_{12}}}Y_2'(2\sqrt{b_{22}s_{12}}) \\ \left[2\sqrt{b_{12}s_{12}}J_2'(2\sqrt{b_{12}s_{12}})-2\nu J_2(2\sqrt{b_{12}s_{12}})\right]\cos\alpha_2 & \left[2\sqrt{b_{12}s_{12}}Y_2'(2\sqrt{b_{12}s_{12}})-2\nu Y_2(2\sqrt{b_{12}s_{12}})\right]\cos\alpha_2 & \left[2\sqrt{b_{22}s_{12}}J_2'(2\sqrt{b_{22}s_{12}})-2\nu J_2(2\sqrt{b_{22}s_{12}})\right]\cos\alpha_2 & \left[2\sqrt{b_{22}s_{12}}Y_2'(2\sqrt{b_{22}s_{12}})-2\nu Y_2(2\sqrt{b_{22}s_{12}})\right]\cos\alpha_2 \end{bmatrix} \tag{13}$$

$$E=\begin{bmatrix} \frac{1}{4s_{21}^2}\left[(2\sqrt{b_{11}s_{21}})^3J_2'(2\sqrt{b_{11}s_{21}})+2\nu(2\sqrt{b_{11}s_{21}})^2J_2(2\sqrt{b_{11}s_{21}})\right] & \frac{1}{4s_{21}^2}((2\sqrt{b_{11}s_{21}})^3Y_2'(2\sqrt{b_{11}s_{21}})+2\nu(2\sqrt{b_{11}s_{21}})^2Y_2(2\sqrt{b_{11}s_{21}})) & \frac{1}{4s_{21}^2}\left[(2\sqrt{b_{21}s_{21}})^3J_2'(2\sqrt{b_{21}s_{21}})+2\nu(2\sqrt{b_{21}s_{21}})^2J_2(2\sqrt{b_{21}s_{21}})\right] & \frac{1}{4s_{21}^2}\left[(2\sqrt{b_{21}s_{21}})^3Y_2'(2\sqrt{b_{21}s_{21}})+2\nu(2\sqrt{b_{21}s_{21}})^2Y_2(2\sqrt{b_{21}s_{21}})\right] \\ \sqrt{\frac{b_{11}}{s_{21}}}J_2'(2\sqrt{b_{11}s_{21}}) & \sqrt{\frac{b_{11}}{s_{21}}}Y_2'(2\sqrt{b_{11}s_{21}}) & \sqrt{\frac{b_{21}}{s_{21}}}J_2'(2\sqrt{b_{21}s_{21}}) & \sqrt{\frac{b_{21}}{s_{21}}}Y_2'(2\sqrt{b_{21}s_{21}}) \\ 0 & 0 & 0 & 0 \\ 0 & 0 & 0 & 0 \end{bmatrix} \tag{14}$$

$$F=\begin{bmatrix} \frac{1}{4s_{12}^2}\left[(2\sqrt{b_{12}s_{12}})^3J_2'(2\sqrt{b_{12}s_{12}})+2\nu(2\sqrt{b_{12}s_{12}})^2J_2(2\sqrt{b_{12}s_{12}})\right] & \frac{1}{4s_{12}^2}\left[(2\sqrt{b_{12}s_{12}})^3Y_2'(2\sqrt{b_{12}s_{12}})+2\nu(2\sqrt{b_{12}s_{12}})^2Y_2(2\sqrt{b_{12}s_{12}})\right] & \frac{1}{4s_{12}^2}\left[(2\sqrt{b_{22}s_{12}})^3J_2'(2\sqrt{b_{22}s_{12}})+2\nu(2\sqrt{b_{22}s_{12}})^2J_2(2\sqrt{b_{22}s_{12}})\right] & \frac{1}{4s_{12}^2}\left[(2\sqrt{b_{22}s_{12}})^3Y_2'(2\sqrt{b_{22}s_{12}})+2\nu(2\sqrt{b_{22}s_{12}})^2Y_2(2\sqrt{b_{22}s_{12}})\right] \\ \sqrt{\frac{b_{12}}{s_{12}}}J_2'(2\sqrt{b_{12}s_{12}}) & \sqrt{\frac{b_{12}}{s_{12}}}Y_2'(2\sqrt{b_{12}s_{12}}) & \sqrt{\frac{b_{22}}{s_{12}}}J_2'(2\sqrt{b_{22}s_{12}}) & \sqrt{\frac{b_{22}}{s_{12}}}Y_2'(2\sqrt{b_{22}s_{12}}) \\ (2\sqrt{b_{12}s_{22}})J_2'(2\sqrt{b_{12}s_{22}})-2\nu J_2(2\sqrt{b_{12}s_{22}}) & (2\sqrt{b_{12}s_{22}})^2Y_2'(2\sqrt{b_{12}s_{22}})-2\nu Y_2(2\sqrt{b_{12}s_{22}}) & (2\sqrt{b_{22}s_{22}})J_2'(2\sqrt{b_{22}s_{22}})-2\nu J_2(2\sqrt{b_{22}s_{22}}) & (2\sqrt{b_{22}s_{22}})Y_2'(2\sqrt{b_{22}s_{22}})-2\nu Y_2(2\sqrt{b_{22}s_{22}}) \\ (2\sqrt{b_{12}s_{22}})^3J_2'(2\sqrt{b_{12}s_{22}})+2\nu(2\sqrt{b_{12}s_{22}})^2J_2(2\sqrt{b_{12}s_{22}}) & (2\sqrt{b_{12}s_{22}})^3Y_2'(2\sqrt{b_{12}s_{22}})+2\nu(2\sqrt{b_{12}s_{22}})^2Y_2(2\sqrt{b_{12}s_{22}}) & (2\sqrt{b_{22}s_{22}})^3J_2'(2\sqrt{b_{22}s_{22}})+2\nu(2\sqrt{b_{22}s_{22}})^2J_2(2\sqrt{b_{22}s_{22}}) & (2\sqrt{b_{22}s_{22}})^3Y_2'(2\sqrt{b_{22}s_{22}})+2\nu(2\sqrt{b_{22}s_{22}})^2Y_2(2\sqrt{b_{22}s_{22}}) \end{bmatrix} \tag{15}$$

The primes indicate differentiation with respect to s. The stability determinant given by Eqs. (11) to (15) is very complicated but gives a simplified result when Poisson's ratio is set equal to zero. It can be argued that solving the determinant of coefficients are usually not sensitive to Poisson's ratio (Seide 1956). However, it is not concluded that the obtained critical load leaves out the effect of Poisson's ratio because the parameters $b_{1,2}$ include the effect of Poisson's ratio in the buckling load (Lackman and Penzien 1960). With this argument, Eqs. (13)-(15) are simplified and we have

$$A=\begin{bmatrix} G_{11}J_2'(2\sqrt{b_{11}s_{11}}) & G_{11}Y_2'(2\sqrt{b_{11}s_{11}}) & G_{12}J_2'(2\sqrt{b_{21}s_{11}}) & G_{12}Y_2'(2\sqrt{b_{21}s_{11}}) \\ G_{21}J_2'(2\sqrt{b_{11}s_{11}}) & G_{21}Y_2'(2\sqrt{b_{11}s_{11}}) & G_{22}J_2'(2\sqrt{b_{21}s_{11}}) & G_{22}Y_2'(2\sqrt{b_{21}s_{11}}) \\ G_{31}J_2'(2\sqrt{b_{11}s_{21}}) & G_{31}Y_2'(2\sqrt{b_{11}s_{21}}) & G_{32}J_2'(2\sqrt{b_{21}s_{21}}) & G_{32}Y_2'(2\sqrt{b_{21}s_{21}}) \\ G_{41}J_2'(2\sqrt{b_{11}s_{21}}) & G_{41}Y_2'(2\sqrt{b_{11}s_{21}}) & G_{42}J_2'(2\sqrt{b_{21}s_{21}}) & G_{42}Y_2'(2\sqrt{b_{21}s_{21}}) \end{bmatrix} \tag{16}$$

$$B=\begin{bmatrix} 0 & 0 & 0 & 0 \\ 0 & 0 & 0 & 0 \\ G_{33}J_2'(2\sqrt{b_{12}s_{12}}) & G_{33}Y_2'(2\sqrt{b_{12}s_{12}}) & G_{34}J_2'(2\sqrt{b_{22}s_{12}}) & G_{34}Y_2'(2\sqrt{b_{22}s_{12}}) \\ G_{43}J_2'(2\sqrt{b_{12}s_{12}}) & G_{43}Y_2'(2\sqrt{b_{12}s_{12}}) & G_{44}J_2'(2\sqrt{b_{22}s_{12}}) & G_{44}Y_2'(2\sqrt{b_{22}s_{12}}) \end{bmatrix} \tag{17}$$

$$E=\begin{bmatrix} G_{51}J_2'(2\sqrt{b_{11}s_{21}}) & G_{51}Y_2'(2\sqrt{b_{11}s_{21}}) & G_{52}J_2'(2\sqrt{b_{21}s_{21}}) & G_{52}Y_2'(2\sqrt{b_{21}s_{21}}) \\ G_{61}J_2'(2\sqrt{b_{11}s_{21}}) & G_{61}Y_2'(2\sqrt{b_{11}s_{21}}) & G_{62}J_2'(2\sqrt{b_{21}s_{21}}) & G_{62}Y_2'(2\sqrt{b_{21}s_{21}}) \\ 0 & 0 & 0 & 0 \\ 0 & 0 & 0 & 0 \end{bmatrix} \tag{18}$$

$$F=\begin{bmatrix} G_{53}J_2'(2\sqrt{b_{12}s_{12}}) & G_{53}Y_2'(2\sqrt{b_{12}s_{12}}) & G_{54}J_2'(2\sqrt{b_{22}s_{12}}) & G_{54}Y_2'(2\sqrt{b_{22}s_{12}}) \\ G_{63}J_2'(2\sqrt{b_{12}s_{12}}) & G_{63}Y_2'(2\sqrt{b_{12}s_{12}}) & G_{64}J_2'(2\sqrt{b_{22}s_{12}}) & G_{64}Y_2'(2\sqrt{b_{22}s_{12}}) \\ G_{23}J_2'(2\sqrt{b_{12}s_{22}}) & G_{23}Y_2'(2\sqrt{b_{12}s_{22}}) & G_{24}J_2'(2\sqrt{b_{22}s_{22}}) & G_{24}Y_2'(2\sqrt{b_{22}s_{22}}) \\ G_{13}J_2'(2\sqrt{b_{12}s_{22}}) & G_{13}Y_2'(2\sqrt{b_{12}s_{22}}) & G_{14}J_2'(2\sqrt{b_{22}s_{22}}) & G_{14}Y_2'(2\sqrt{b_{22}s_{22}}) \end{bmatrix} \tag{19}$$

Where G_{ij}s are the coefficients of differentiated Bessel functions described as

$$\begin{array}{llll} G_{11}=(2\sqrt{b_{11}s_{11}})^3 & G_{12}=(2\sqrt{b_{21}s_{11}})^3 & G_{13}=(2\sqrt{b_{12}s_{22}})^3 & G_{14}=(2\sqrt{b_{22}s_{22}})^3 \\ G_{21}=2\sqrt{b_{11}s_{11}} & G_{22}=2\sqrt{b_{21}s_{11}} & G_{23}=2\sqrt{b_{12}s_{22}} & G_{24}=2\sqrt{b_{22}s_{22}} \\ G_{31}=\dfrac{b_{11}^2}{2\sqrt{b_{11}s_{21}}} & G_{32}=\dfrac{b_{21}^2}{2\sqrt{b_{21}s_{21}}} & G_{33}=-\dfrac{b_{12}^2}{2\sqrt{b_{12}s_{12}}} & G_{34}=-\dfrac{b_{22}^2}{2\sqrt{b_{22}s_{12}}} \\ G_{41}=2\sqrt{b_{11}s_{21}}\cos\alpha_1 & G_{42}=2\sqrt{b_{21}s_{21}}\cos\alpha_1 & G_{43}=-2\sqrt{b_{12}s_{12}}\cos\alpha_2 & G_{44}=-2\sqrt{b_{22}s_{12}}\cos\alpha_2 \\ G_{51}=\dfrac{(2\sqrt{b_{11}s_{21}})^3}{4s_{21}^2} & G_{52}=\dfrac{(2\sqrt{b_{21}s_{21}})^3}{4s_{21}^2} & G_{53}=-\dfrac{(2\sqrt{b_{12}s_{12}})^3}{4s_{12}^2} & G_{54}=-\dfrac{(2\sqrt{b_{22}s_{12}})^3}{4s_{12}^2} \\ G_{61}=\sqrt{\dfrac{b_{11}}{s_{21}}} & G_{62}=\sqrt{\dfrac{b_{21}}{s_{21}}} & G_{63}=-\sqrt{\dfrac{b_{12}}{s_{12}}} & G_{64}=-\sqrt{\dfrac{b_{22}}{s_{12}}} \end{array} \tag{20}$$

By solving the determinant of coefficients Eq. (11) we have

$$
\begin{aligned}
&\{(G_{71}G_{74}-G_{72}G_{73})\times(G_{12}G_{21}-G_{11}G_{22})\times(G_{14}G_{23}-G_{13}G_{24})\times(G_{54}G_{63}-G_{53}G_{64})\times\\
&\left[J_2'(2\sqrt{b_{11}s_{11}})Y_2'(2\sqrt{b_{11}s_{21}})-J_2'(2\sqrt{b_{11}s_{21}})Y_2'(2\sqrt{b_{11}s_{11}})\right]\times\left[J_2'(2\sqrt{b_{12}s_{12}})Y_2'(2\sqrt{b_{12}s_{22}})-J_2'(2\sqrt{b_{12}s_{22}})Y_2'(2\sqrt{b_{12}s_{12}})\right]\times\\
&\left[J_2'(2\sqrt{b_{21}s_{11}})Y_2'(2\sqrt{b_{21}s_{21}})-J_2'(2\sqrt{b_{21}s_{21}})Y_2'(2\sqrt{b_{21}s_{11}})\right]\times\left[J_2'(2\sqrt{b_{22}s_{12}})Y_2'(2\sqrt{b_{22}s_{22}})-J_2'(2\sqrt{b_{22}s_{22}})Y_2'(2\sqrt{b_{22}s_{12}})\right]\}=0
\end{aligned}
\tag{21}
$$

where

$$
\begin{aligned}
G_{71}&=(G_{31}+\frac{G_{34}G_{53}G_{61}-G_{33}G_{54}G_{61}-G_{34}G_{51}G_{63}+G_{33}G_{51}G_{64}}{G_{54}G_{63}-G_{53}G_{64}})\\
G_{72}&=(G_{32}+\frac{G_{34}G_{53}G_{62}-G_{33}G_{54}G_{62}-G_{34}G_{52}G_{63}+G_{33}G_{52}G_{64}}{G_{54}G_{63}-G_{53}G_{64}})\\
G_{73}&=(G_{41}+\frac{G_{44}G_{53}G_{61}-G_{43}G_{54}G_{61}-G_{44}G_{51}G_{63}+G_{43}G_{51}G_{64}}{G_{54}G_{63}-G_{53}G_{64}})\\
G_{74}&=(G_{42}+\frac{G_{44}G_{53}G_{62}-G_{43}G_{54}G_{62}-G_{44}G_{52}G_{63}+G_{43}G_{52}G_{64}}{G_{54}G_{63}-G_{53}G_{64}})
\end{aligned}
\tag{22}
$$

Finally, for obtaining the buckling load of two joined shells we must have

$$
\begin{cases}
J_2'(2\sqrt{b_{11}s_{11}})Y_2'(2\sqrt{b_{11}s_{21}})-J_2'(2\sqrt{b_{11}s_{21}})Y_2'(2\sqrt{b_{11}s_{11}})=0\\
J_2'(2\sqrt{b_{21}s_{11}})Y_2'(2\sqrt{b_{21}s_{21}})-J_2'(2\sqrt{b_{21}s_{21}})Y_2'(2\sqrt{b_{21}s_{11}})=0
\end{cases}
\tag{23}
$$

$$
\begin{cases}
J_2'(2\sqrt{b_{12}s_{12}})Y_2'(2\sqrt{b_{12}s_{22}})-J_2'(2\sqrt{b_{12}s_{22}})Y_2'(2\sqrt{b_{12}s_{12}})=0\\
J_2'(2\sqrt{b_{22}s_{12}})Y_2'(2\sqrt{b_{22}s_{22}})-J_2'(2\sqrt{b_{22}s_{22}})Y_2'(2\sqrt{b_{22}s_{12}})=0
\end{cases}
\tag{24}
$$

Eqs. (23) and (24) are cross products of Bessel functions which arise in solving the Bessel equations subject to Neumann boundary conditions. The solution of Eqs. (23) and (24) can be expressed as

$$
\begin{cases}
2\sqrt{b_{11,12}s_{11}}=X_{n1}(\sqrt{\dfrac{s_{21}}{s_{11}}})\\
2\sqrt{b_{12,22}s_{12}}=X_{n2}(\sqrt{\dfrac{s_{22}}{s_{12}}})
\end{cases}
\tag{25}
$$

where X_{n1} and X_{n2} are the roots of Bessel Eqs. (23) and (24). The Eq. (25) expands to

$$
\begin{cases}
\dfrac{P_1\sqrt{3(1-\nu_1^2)}}{2E_1h_1^2\pi\cos^2\alpha_1}=\dfrac{1}{2}\left[\dfrac{X_{n1}^2}{\dfrac{8s_{11}}{h_1}\sqrt{3(1-\nu_1^2)}\cot\alpha_1}+\dfrac{\dfrac{8s_{11}}{h_1}\sqrt{3(1-\nu_1^2)}\cot\alpha_1}{X_{n1}^2}\right]\\
\dfrac{P_2\sqrt{3(1-\nu_2^2)}}{2E_2h_2^2\pi\cos^2\alpha_2}=\dfrac{1}{2}\left[\dfrac{X_{n2}^2}{\dfrac{8s_{12}}{h_2}\sqrt{3(1-\nu_2^2)}\cot\alpha_2}+\dfrac{\dfrac{8s_{12}}{h_2}\sqrt{3(1-\nu_2^2)}\cot\alpha_2}{X_{n2}^2}\right]
\end{cases}
\tag{26}
$$

The values of X_{n1} and X_{n2} are to be selected so that it yields the lowest value of P. As the right side of equalities in Eq. (26) is in $(a+\frac{1}{a})$ form, the minimization of two similar expressions in (26) leads to

$$\begin{cases} P_{cr1} = \dfrac{2E_1h_1^2\pi\cos^2\alpha_1}{\sqrt{3(1-\nu_1^2)}} \\ P_{cr2} = \dfrac{2E_2h_2^2\pi\cos^2\alpha_2}{\sqrt{3(1-\nu_2^2)}} \end{cases} \tag{27}$$

which is similar to solution reported by Seide (1956). Finally, it can be argued that the buckling load of two joined conical shells is obtained from the expressions of Eq. (27). It presents that the buckling load of a structure consisting of two joined conical shells is equal to the minimum buckling load of each cone, individually. The dimension of buckling load is 'Newton (N)' in SI unit.

4. Results

To examine the accuracy of the present analysis, some comparisons are made against the results obtained by finite element (FE) approach.

The FE analysis is carried out with ANSYS software by using 2-node axisymmetric shell element. Using this element, we make a one dimensional model subjected to axial compression. The model has 300 elements and the convergence of the results is checked. Boundary conditions are simply-supported in both ends exactly the same as what is done in analytical approach, i.e., Eq. (8), and linear buckling load of joined shells with various semi-vertex angles is investigated. The Block-Lanczos method, which is a variation of the classical Lanczos algorithm, is used to solve eigenvalue extraction. In this algorithm, the Lanczos recursions are performed using a block of vectors whereas in classical Lanczos method a single vector is used (Lawrence 2012). Details about Lanczos method and its application to the finite element method can be found in (Grimes *et al*. 1994, Cullum and Willoughby 2002).

In Table 1, the values of the critical axial load for two joined isotropic truncated conical shells obtained from FE analysis are compared with present results. The properties for conical shells are

$$\begin{aligned} &E_1 = E_2 = 29\,000 \text{ ksi} \\ &\nu_1 = \nu_2 = 0.3 \\ &h_1 = h_2 = 0.005 \text{ in} \\ &L_1 = L_2 = L \\ &R = 1 \quad \text{in} \end{aligned} \tag{27}$$

It can be seen that the present results are in good agreement with results of FE analysis for long cones (i.e., higher values of L/R) and the errors arise when the second cone semi-vertex is close to 90°. Fig. 2 shows the variation of buckling load of joined cones with respect to α_2. The material properties are as mentioned above, L/R=1 and α_1=30°. The results show that Eq. (27) can successfully predict the buckling load of joined shells.

Table 1 Axial buckling load (N) of two joined conical shells compared with FE results

		L/R=0.5			L/R=1			L/R=2		
α_1	α_2	FE	Present	Error (%)	FE	Present	Error (%)	FE	Present	Error (%)
	-75	854.50	821.59	3.85	808.69	821.59	1.60			
	-60	3146.23	3066.16	2.54	3054.15	3066.16	0.39			
	-45	6262.65	6131.87	2.09	6130.54	6131.87	0.02			
	-30	9354.61	9198.03	1.67	9210.04	9198.03	0.13			
0	0	12250.40	12263.75	0.11	12245.95	12263.75	0.15	12236.61	12263.75	0.22
	30	9431.12	9198.03	2.47	9272.76	9198.03	0.81	9217.16	9198.03	0.21
	45	6357.84	6131.87	3.55	6207.94	6131.87	1.23	6155.45	6131.87	0.38
	60	3229.85	3066.16	5.07	3126.12	3066.16	1.92	3085.73	3066.16	0.63
	75	918.11	821.59	10.51	848.28	821.59	3.15	833.15	821.59	1.39
	-75	881.19	821.59	6.76	833.15	821.59	1.39	812.69	821.59	1.09
	-60	3185.82	3066.16	3.76	3090.62	3066.16	0.79	3060.38	3066.16	0.19
	-45	6297.79	6131.87	2.63	6170.57	6131.87	0.63	6131.87	6131.87	0.00
	-30	9251.86	9198.03	0.58	9234.95	9198.03	0.40	9194.92	9198.03	0.03
30	0	9254.53	9198.03	0.61	9254.53	9198.03	0.61	9205.15	9198.03	0.08
	30	9190.92	9198.03	0.08	9201.59	9198.03	0.04	9186.02	9198.03	0.13
	45	6387.20	6131.87	4.00	6227.07	6131.87	1.53	6168.79	6131.87	0.60
	60	3244.09	3066.16	5.48	3140.44	3066.16	2.37	3097.30	3066.16	1.01
	75	920.34	821.59	10.73	863.84	821.59	4.89	838.49	821.59	2.02
	-75	888.75	821.59	7.56	838.49	821.59	2.02	825.59	821.59	0.48
	-60	3128.88	3066.16	2.00	3100.86	3066.16	1.12	3071.94	3066.16	0.19
	-45	3193.82	3066.16	4.00	3106.64	3066.16	1.30	3075.95	3066.16	0.32
	-30	3196.05	3066.16	4.06	3107.53	3066.16	1.33	3075.95	3066.16	0.32
60	0	3196.94	3066.16	4.09	3108.42	3066.16	1.36	3075.95	3066.16	0.32
	30	3196.94	3066.16	4.09	3108.42	3066.16	1.36	3075.95	3066.16	0.32
	45	3192.49	3066.16	3.96	3106.64	3066.16	1.30	3075.95	3066.16	0.32
	60	3064.82	3066.16	0.04	3068.38	3066.16	0.07	3063.94	3066.16	0.07
	75	921.67	821.59	10.86	866.07	821.59	5.14	839.82	821.59	2.17

The axisymmetric mode shapes of joined shells obtained from present study and FE analysis for L/R=1 and α_1=45°and α_2=30° are shown in the left and right sides of Fig. 3. As can be seen, the mode shapes of joined shells have the same behavior and it can be concluded from Table 1 and Figs. 2 and 3 that the results of present study are in proper accordance with FE analysis in both buckling value and mode shapes. In addition, it is seen that although the buckling load of joined shells is equal to the minimum buckling load of the separated shells (not affected by joining them), the mode shape of joined shells is affected by joining them due to Eq. (9) and we have no deformation discontinuity in mode shapes at the intersection of shells.

The variation of axial buckling load versus semi-vertex cone angles is shown in Fig. 4. It can be observed that the maximum buckling load of joined shell occurs when both semi-vertex angles are zero (i.e., cylindrical shells) and the buckling load approaches zero when one of the semi-vertex angles reaches 90° (i.e., annular plate). The variation of buckling load is similar to Fig. 2 in any specific value of α_1.

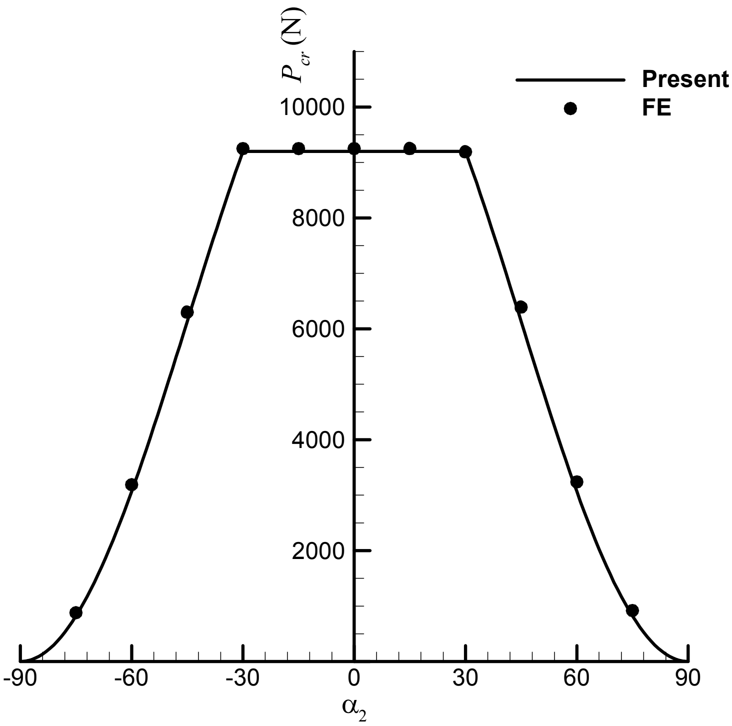

Fig. 2 Variation of axial buckling load of two joined conical shells versus α_2: FE and present results (α_1=30°, L/R=1)

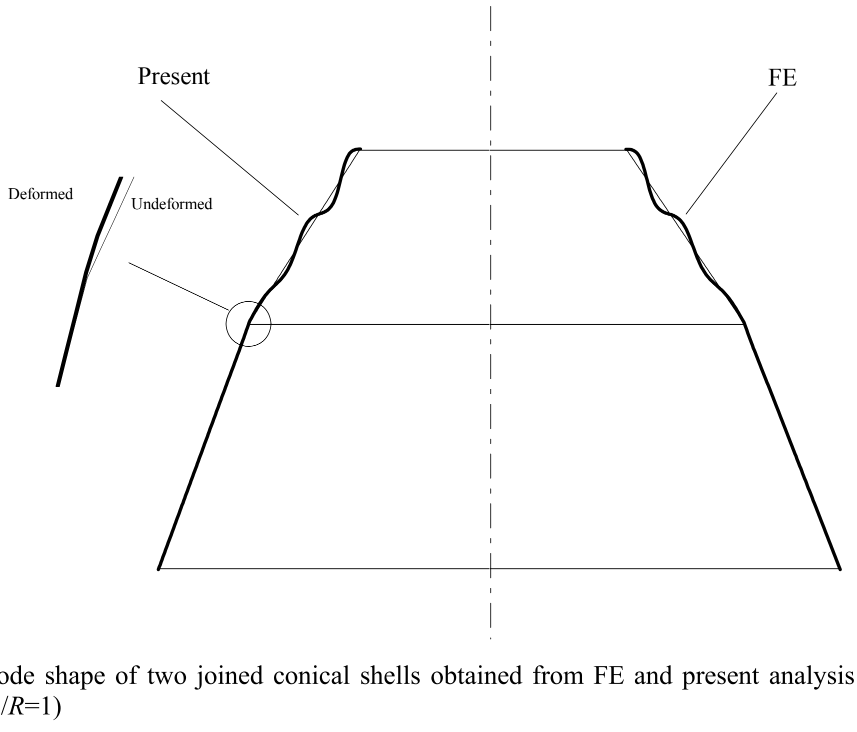

Fig. 3 Mode shape of two joined conical shells obtained from FE and present analysis (α_1=45°, α_2=30°, L/R=1)

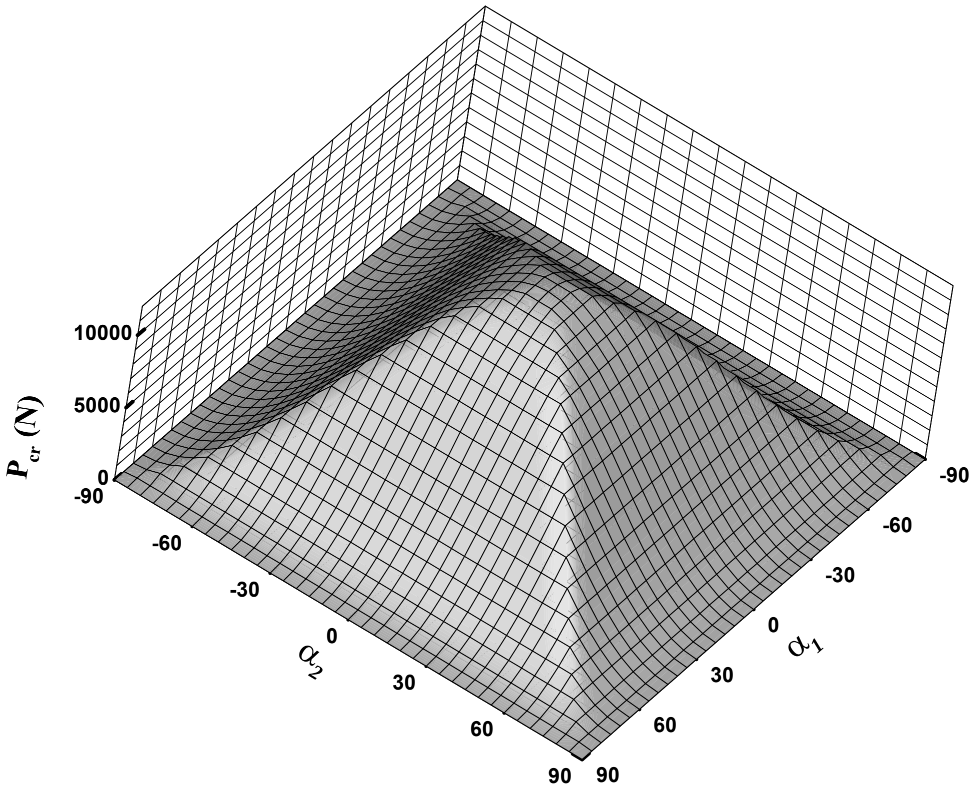

Fig. 4 Variation of axial buckling load of two joined conical shells versus semi-vertex cone angles α_1 and α_2

5. Application of the results

The obtained simple expression can be used in designing procedure to give a primary estimation about stability of joined shells against axial compression. In this section, the application of this expression will be discussed more.

5.1 Optimized weight of joined shells

As one of applications of this study, results may be used to find the best geometry of joined shells to have minimum weight when the joined shells are subjected to axial compression. As an explanation, assume two joined conical shells subjected to axial load. Minimum weight of the structure can be achieved when the two joined shells have the same buckling loads. It means that both conical shells buckle at the same load and the material is used in the most efficient condition. This implies that

$$h_2 = h_1 \frac{\cos\alpha_1}{\cos\alpha_2}\left[\frac{E_1}{E_2}\sqrt{\frac{1-\nu_2^{\,2}}{1-\nu_1^{\,2}}}\right]^{\frac{1}{2}} \tag{27}$$

For a numerical example, consider the case of two joined conical shells with the minimum

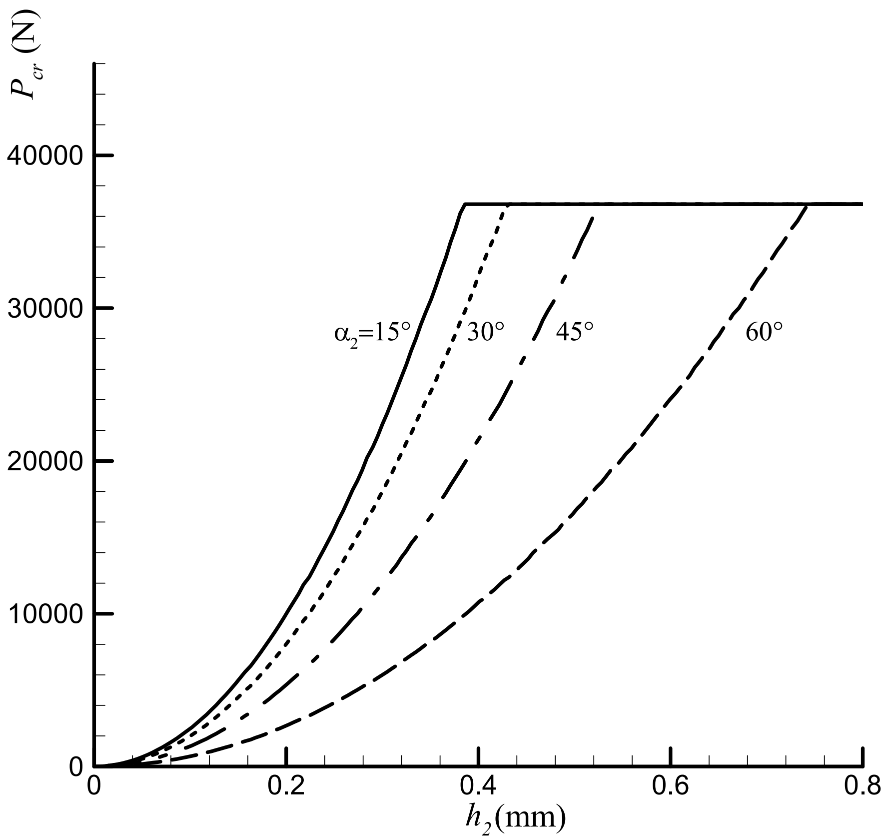

Fig. 5 Variation of axial buckling load of joined steel and aluminum conical shells versus aluminum cone thickness (α_1=30°, L/R=1 and h_1=0.254 mm)

weight to bear axial load. The first cone is made up of steel with semi-vertex angle of 30° and second is from aluminum with semi-vertex angle of 45°. The numerical values are

$$\begin{array}{lll} E_1 = 200 \text{ GPa}, & E_2 = 69 \text{ GPa}, & h_1 = 0.254 \text{ mm} \\ \nu_1 = 0.3, & \nu_2 = 0.35 & \end{array} \qquad (28)$$

Using Eq. (27) the minimum thickness of aluminum cone becomes 0.533 mm. The variation of buckling load versus h_2 for this case is shown in Fig. 5. As can be seen, the minimum second shell thickness is the intersection of parabolic and horizontal sections for each semi-vertex angles.

5.2 Range of validity

Although the Eq. (27) is derived using axisymmetric assumption for buckling of joined shells and the circumferential modes are neglected, it is applicable in a wide range of engineering geometries of joined shells. To use this expression in shell design against axial load, it is necessary to show the range of geometries that Eq. (27) is utilizable. To this end, an extensive area of geometries of joined shells was analyzed using finite element calculation. The 2-D 8-node shell element with 6 degrees of freedom is used to analyze the joined shells. This element is suitable for analyzing thin to moderately-thick shell structures by using first order shear deformation theory. It is to be noted that here, a general analysis (i.e., the analysis is not with axisymmetric assumptions) is done with finite element analysis. The method of solution is exactly the same as the way described in Sec. 4. At the end, the linear (bifurcation) buckling load of the specified joined shells (P_{FE}) are extracted and the discrepancy between those values and the values obtained from Eq. (27) (P_{AN}) is

$$e = \frac{P_{AN} - P_{FE}}{P_{FE}} \times 100 \tag{31}$$

where e is the discrepancy of the results.

For the sake of simplicity, it is assumed that the joined shells have the same thicknesses (h_1=h_2=h) and manufactured from the same material. The L_1/R and L_2/R are changed from 0.1 to 1.5, R/h is studied in the range of 20 to 200 and α_1 and α_2 are between 0° to 60°. The maximum value selected for semi-vertex angles is the limit value that is commonly adopted in the buckling analysis and design of conical shells in linear (bifurcation) instability (e.g., see ECCS (Rotter and Schmidt 2008)). Beyond such a value, aspects related to nonlinear instabilities (like snap-through phenomena, large deformation and rotation, etc.) might be more relevant than those related to bifurcation instability.

It is observed that the values of the e is less than 5% for the region that the values of geometric parameters are as follows

$$\begin{cases} 15° \le \alpha_1 \le \alpha_2 \le 35° \\ 0.6 \le \dfrac{L_1}{R}, \dfrac{L_2}{R} \le 1.5 \\ 30 \le \dfrac{R}{h} \le 100 \end{cases} \tag{32}$$

As can be seen, there is a wide range of joined cone geometries that the Eq. (27) is applicable. This is a very good expression for preliminary design of joined shells under axial compression to show that if it is stable or not. In this region, the buckling load of a structure with two joined conical shells can be obtained using Eq. (27) and ensure that the discrepancy between this value and the actual buckling load is less than 5%. It is necessary to be noted that for the geometries outside this region, the Eq. (32) doesn't mean that the difference between predicted and FE buckling loads are more than 5%, but, it might be more or less than this value.

6. Conclusions

The axisymmetric buckling load of two joined isotropic conical shells under axial compression is studied. The governing equations for the conical shells are obtained and solved with an analytical approach. A closed form solution for buckling load of joined conical shells is obtained. The results have good agreement with FE numerical results in both buckling load and mode shapes. The analytical result supports the following conclusions:

The axisymmetric buckling load of a structure consisting of two joined truncated cones under axial compression is equal to the minimum buckling load for each of the truncated cones alone. This means that in this case, each single cone is involved separately in the buckling under the axial load.

Results of this study may be used to design and optimize a structure consisting of two conical shells. To do this, one must obtain the geometrical and material characteristics of each cone so that the buckling load is the same in two conical shells. This approach results in minimum weight of joined conical shells under axial load. In addition, it is shown that the result of the present study is applicable in a wide range of joined shell geometries.

References

Anwen, W. (1998), "Stresses and stability for the cone-cylinder shells with toroidal transition", *Int. J. Press. Vess. Pip.*, **75**(1), 49-56.

Bushnell, D. and Galletly, G.D. (1974), "Comparisons of test and theory for nonsymmetric elastic-plastic buckling of shells of revolution", *Int. J. Solid. Struct.*, **10**(11), 1271-1286.

Civalek, Ö. (2013), "Vibration analysis of laminated composite conical shells by the method of discrete singular convolution based on the shear deformation theory", *Compos. Part B*, **45**(1), 1001-1009.

Civalek, Ö. and Gürses, M. (2009), "Free vibration analysis of rotating cylindrical shells using discrete singular convolution technique", *Int. J. Press. Vess. Pip.*, **86**(10), 677-683.

Cullum, J.K. and Willoughby, R.A. (2002), *Lanczos Algorithms for Large Symmetric Eigenvalue Computations: Vol. 1: Theory*, SIAM

Flores, F.G. and Godoy, L.A. (1991), "Post-buckling of elastic cone-cylinder and sphere-cylinder complex shells", *Int. J. Press. Vess. Pip.*, **45**(2), 237-258.

Grimes, R.G., Lewis, J.G. and Simon, H.D. (1994), "A shifted block Lanczos algorithm for solving sparse symmetric generalized eigenproblems", *SIAM J. Matrix Anal. Appl.*, **15**(1), 228-272.

Gupta, N., Sheriff, N.M. and Velmurugan, R. (2006), "A study on buckling of thin conical frusta under axial loads", *Thin Wall. Struct.*, **44**(9), 986-996.

Hafeez, G., El Ansary, A. and El Damatty, A. (2010), "Stability of combined imperfect conical tanks under hydrostatic loading", *J. Constr. Steel Res.*, **66**(11), 1387-1397.

Hui, D. (1988), "Effects of shear loads on vibration and buckling of antisymmetric cross-ply cylindrical panels", *Int. J. Nonlin. Mech.*, **23**(3), 177-187.

Kamat, S., Ganapathi, M. and Patel, B.P. (2001), "Analysis of parametrically excited laminated composite joined conical-cylindrical shells", *Comput. Struct.*, **79**(1), 65-76.

Kouchakzadeh, M.A. and Shakouri, M. (2014), "Free vibration analysis of joined cross-ply laminated conical shells", *Int. J. Mech. Sci.*, **78**, 118-125.

Lackman, L. and Penzien, J. (1960), "Buckling of circular cones under axial compression", *J. Appl. Mech.*, **27**, 458.

Lawrence, K.L. (2012), ANSYS Tutorial: Release 14, SDC Publications

Patel, B.P., Nath, Y. and Shukla, K.K. (2006), "Nonlinear thermo-elastic buckling characteristics of cross-ply laminated joined conical-cylindrical shells", *Int. J. Solid. Struct.*, **43**(16), 4810-4829.

Patel, B.P., Shukla, K.K. and Nath, Y. (2005), "Thermal postbuckling analysis of laminated cross-ply truncated circular conical shells", *Compos. Struct.*, **71**(1), 101-114.

Patel, B.P., Singh, S. and Nath, Y. (2008), "Postbuckling characteristics of angle-ply laminated truncated circular conical shells", *Commun. Nonlin. Sci. Numer. Simul.*, **13**(7), 1411-1430.

Ross, C.T.F., Little, A.P.F. and Adeniyi, K.A. (2005), "Plastic buckling of ring-stiffened conical shells under external hydrostatic pressure", *Ocean Eng.*, **32**(1), 21-36.

Ross, C.T.F., Sawkins, D. and Johns, T. (1999), "Inelastic buckling of thick-walled circular conical shells under external hydrostatic pressure", *Ocean Eng.*, **26**(12), 1297-1310.

Rotter, J.M. and Schmidt, H. (2008), *ECCS TWG 8.4. Buckling of steel shells*, 5th Edition, European Convention for Constructional Steelwork, Brussels.

Seide, P. (1956), "Axisymmetrical buckling of circular cones under axial compression", *J. appl. Mech*,

23(4), 625-628.
Seide, P. (1956), "Axisymmetrical buckling of circular cones under axial compression", *J Appl. Mech*., **23**(4), 625-628.
Shadmehri, F., Hoa, S.V. and Hojjati, M. (2012), "Buckling of conical composite shells", *Compos. Struct*., **94**(2), 787-792.
Simitses, G.J. (1996), "Buckling of moderately thick laminated cylindrical shells: a review", *Compos. Part B*, **27**(6), 581-587.
Sofiyev, A.H. (2003), "The buckling of an orthotropic composite truncated conical shell with continuously varying thickness subject to a time dependent external pressure", *Compos. Part B*, **34**(3), 227-233.
Sofiyev, A.H. (2007), "The buckling of functionally graded truncated conical shells under dynamic axial loading", *J. Sound Vib*., **305**(4-5), 808-826.
Sofiyev, A.H. (2010), "The buckling of FGM truncated conical shells subjected to combined axial tension and hydrostatic pressure", *Compos. Struct*., **92**(2), 488-498.
Sofiyev, A.H. (2011), "Influence of the initial imperfection on the non-linear buckling response of FGM truncated conical shells", *Int. J. Mech. Sci*., **53**(9), 753-761.
Sofiyev, A.H. (2011), "Non-linear buckling behavior of FGM truncated conical shells subjected to axial load", *Int. J. Nonlin. Mech*., **46**(5), 711-719.
Tani, J. and Yamaki, N. (1970), "Buckling of truncated conical shells under axial compression", *AIAA J*., **8**, 568-571.
Teng, J.G. (1996), "Elastic buckling of cone-cylinder intersection under localized circumferential compression", *Eng. Struct*., **18**(1), 41-48.
Teng, J.G. and Barbagallo, M. (1997), "Shell restraint to ring buckling at cone-cylinder intersections", *Eng. Struct*., **19**(6), 425-431.
Teng, J.G. and Ma, H.-W. (1999), "Elastic buckling of ring-stiffened cone-cylinder intersections under internal pressure", *Int. J. Mech. Sci*., **41**(11), 1357-1383.
Ventsel, E. and Krauthammer, T. (2001), *Thin plates and shells: theory, analysis, and applications*, Marcel Dekker.
Zhao, Y. and Teng, J.G. (2003), "A stability design proposal for cone-cylinder intersections under internal pressure", *Int. J. Press. Vess. Pip*., **80**(5), 297-309.
Zingoni, A. (2002), "Discontinuity effects at cone-cone axisymmetric shell junctions", *Thin Wall. Struct*., **40**(10), 877-891.
Zingoni, A. (2004), "On analytical solutions for liquid-filled non-shallow conical shell assemblies", *J. South African Inst. Civil Eng*., **46**(3), 10.

CC